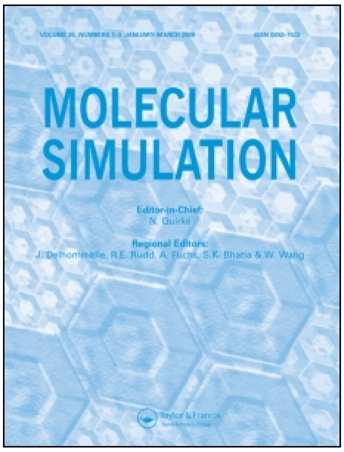

Molecular Simulation
Publication details, including instructions for authors and subscription information:
http://www.informaworld.com/smpp/title~content=t713644482

Molecular modelling of N,N-disubstituted hydrazine phosphorus-containing dendrimers of the fourth generation

Ahmed I. Abou-Kandil[a]; Wolfgang Knoll[a]
[a] Max-Planck Institute for Polymer Research, Mainz, Germany

To cite this Article Abou-Kandil, Ahmed I. and Knoll, Wolfgang(2008) 'Molecular modelling of N,N-disubstituted hydrazine phosphorus-containing dendrimers of the fourth generation', Molecular Simulation, 34: 10, 1289 — 1295
To link to this Article: DOI: 10.1080/08927020801961468
URL: http://dx.doi.org/10.1080/08927020801961468

Molecular Simulation
Vol. 34, Nos. 10–15, September–December 2008, 1289–1295

Molecular modelling of N,N-disubstituted hydrazine phosphorus-containing dendrimers of the fourth generation

Ahmed I. Abou-Kandil* and Wolfgang Knoll

Max-Planck Institute for Polymer Research, Mainz, Germany

(*Received 21 November 2007; final version received 4 February 2008*)

Dendritic polymers are regarded as highly branched regular three-dimensional monodisperse macromolecules with a branch occurring at each monomer unit. Our present study looks into more details in the molecular structure of globular N,N-disubstituted hydrazine phosphorus-containing dendrimers of the fourth generation having 96 terminal groups with either cationic $[G_4(NH^+Et_2Cl^-)_{96}]$ ($\mathbf{G_4^+}$) or anionic $[G_4(CHCOO^-Na^+)_{96}]$ ($\mathbf{G_4^-}$) character. We show that the behaviour of those dendrimers in water leads to the formation of a branched, star-like structure, yet this structure is not completely spherical as previously thought. This finding can explain the differences in thickness of dendrimer thin films produced by Layer-by-Layer deposition. The dendrimers were built, their behaviour in water was determined and the energy minimisation of the system was carried out using computing routines contained within the Materials Studio software.

Keywords: dendrimers; molecular simulation; amorphous cell

1. Introduction

Dendritic polymers, referred mostly as dendrimers are highly branched regular three-dimensional monodisperse macromolecules with a branch occurring at each monomer unit. Large dendrimers adopt a globular shape. They are characterised by the presence of a large number of functional groups on the surface, which result in solubility, viscosity and thermal behaviours different from those of more classical polymers. They are also characterised by the presence of internal cavities, which can be functionalised, and by a core that does or does not bear functional groups. There are several dendrimers prepared in many different synthetic routes order to achieve certain electronic and/or magnetic properties [1–8]. The general structure of those dendrimers is schematically represented in Figure 1.

The increase in the number of branches and the variety of the core structure also controls the architecture of these dendrimers. It affects not only the chemical properties but also the physical properties in terms of rigidity of the overall structure and/or its ability to interact with electric or magnetic fields.

Several types of dendrimers generations 2, 3 and 4 have been synthesised especially to carry either a positive or negative charge on their outer surface, finding applications in Layer-by-Layer (LbL) assembly of supramolecular structures [9–14].

The alternate deposition of G_4^-/G_4^+ by the LbL deposition was successfully demonstrated and has shown a monotonous increase in film thickness as a function of the number of bilayers. The composite multilayers comprised of these shape persistent dendrimers and nanocrystals could be utilised as nanostructured building blocks with excellent control over their porosity, functionality and dimension [13,14].

The multi-layers comprised of pure dendrimers were characterised by electrochemistry to examine the permeability properties using $[Fe(CN)_6]^{3-/4-}$ as the redox couple. None of the previous experimental studies touched the modelling of such massive dendritic polymers or elaborated their behaviour in water, which is crucial to the LbL deposition both on flat Gold surface and/or functionalised Alumina surfaces.

Previous modelling studies done on dendrimers showed that charged and uncharged poly(amidoamine) PAMAM dendrimers strongly adsorb to mica surfaces, resulting in deformation of the molecules [16]. Modelling of other dendrimer structures shows hydrogen bonding upon aggregation, although in the minimum energy conformation such hydrogen bonds did not exist [17]. Modelling also helped to assign proton and carbon resonances of first- and second-generation phenol-terminated carbosilane dendrimers and the second generation of the analogous titanium-ended carbosilane dendrimer [18] and to reveal the structure of stilbenoid dendrimers of third generation by the help of small angle X-ray scattering [19]. The use of unsymmetrical dendrimers was demonstrated to provide nanoscale

---

*Corresponding author. Email: aia_23@yahoo.co.uk

ISSN 0892-7022 print/ISSN 1029-0435 online

DOI: 10.1080/08927020801961468
http://www.informaworld.com

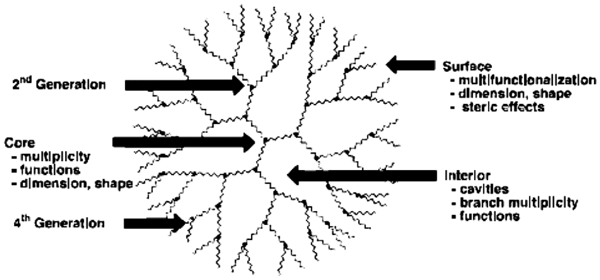

Figure 1. Schematic representation of a fourth generation dendrimer.

platforms for design of bimolecular guest binding receptors [20] and a promising vehicle for intracellular delivery of low-solubility drugs [21].

Several modelling studies of dendritic polymers dealt with "self assembly" of those polymers [22–27] or the properties and applications of different dendrimers in biological and pharmaceutical applications [28–32].

Our present study looks in more detail at the molecular structure of globular N,N-disubstituted hydrazine phosphorus-containing dendrimers of the fourth generation having 96 terminal groups with either cationic [$G_4(NH^+Et_2Cl^-)_{96}$] (G_4^+) or anionic [$G_4(CHCOO^- Na^+)_{96}$] (G_4^-) character. The chemical structure of both dendrimers is illustrated in Figure 2.

2. Results and molecular modelling procedure

Materials Studio® software provided by Accelrys has been used to model the structure of such a massive dendrimer. Other software provided by the same company has been used successfully in modelling the intermediate smectic mesophase in polyethylene terephthalate [33]. The software has also been used to model inclusion of drugs [34], drug delivery [35], calculation of radius of gyration of dendrimers [36,37] and calculating properties of supramolecular structures [38,39].

(1) The *builder* in Materials Studio was used to build the G_4^+ and G_4^- dendrimers under investigation. The seed structure was built separately in a 3D atomistic document. The correct number of generations is constructed using the building fragments in order to build the G_4 dendrimers. Connection points were clearly indicated on the dendrimer seed and fragment. The new dendrimers were then created and viewed in 3D atomistic document.

(2) Finally the terminating fragment was built carrying either carboxylic acid or a tertiary amide group and connected to the building fragments in order to create the correct structure of the dendrimer carrying either 96 negative or positive charges respectively.

(3) The structure resulting from initial dendrimers were "*cleaned*" to tidy up the geometry. This is not an energy minimisation, but, instead, uses a look-up table of standard bond lengths and angles to give a first approximation to the correct geometry of the modelled dendrimers. The structure of the seed, building fragment, positive and negative termination fragments, as well as the overall structure of the positively and negatively charged dendrimers, are illustrated in Figure 3. We emphasise here the planar structure of the N_3P_3 core (Figure 3(a)), as well as the N—P bond in the Building fragment (Figure 3(b)).

(4) In order to add water to the system, an *"amorphous cell"* is constructed where one dendrimer (to reduce the simulation time) is added in a confined space with a certain number of water molecules. The number of water molecules used in the simulations discussed here ranged between 1000 and 2000 water molecules. This helped in reducing the computation time limiting the total number of atoms contained in the system ~10,000.

(5) Amorphous cells were constructed so that the end density of the resulting cell is 1. This was done by adjusting the cell dimensions and the number of water molecules. Adjusting the density value corresponds to the actual density values obtained

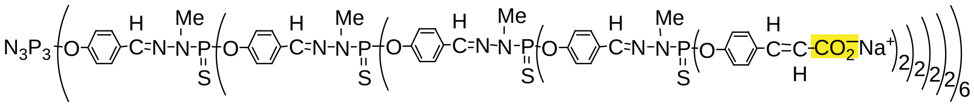

$G_4(COO^-)_{96}$

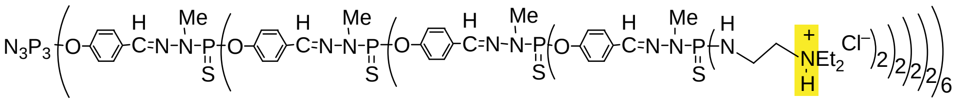

$G_4(NH^+)_{96}$

Figure 2. Chemical structure of the positively and negatively charged dendrimers.

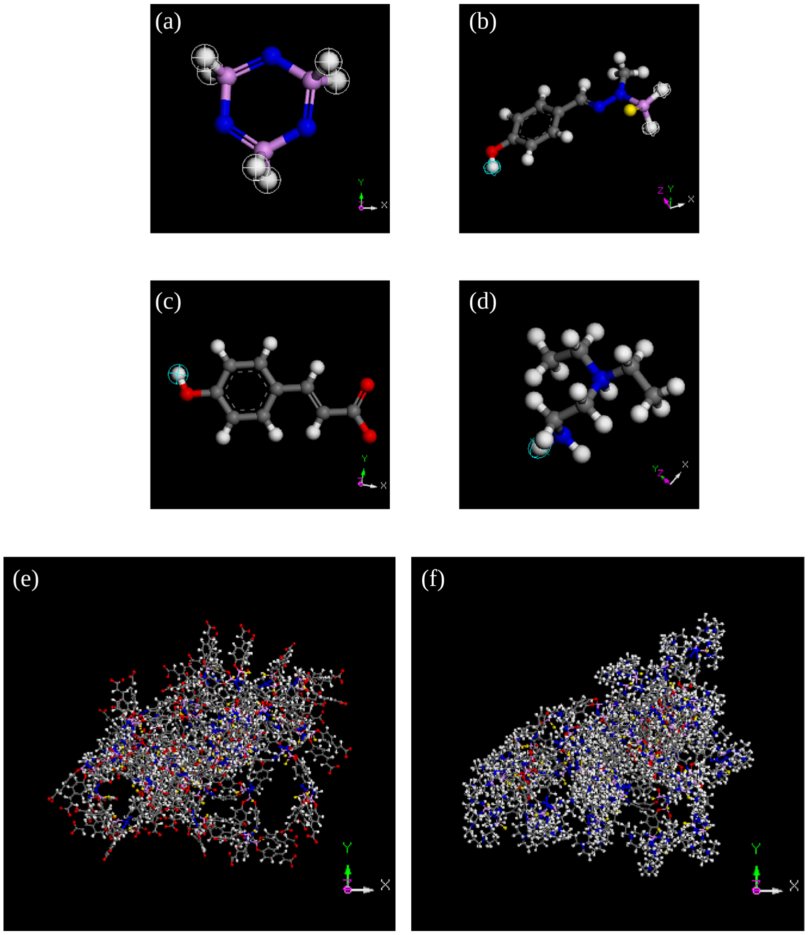

Figure 3. Structure of the (a) N_3P_3 Building core, (b) Building fragment, (c) negatively charged terminating fragment, (d) positively charged terminating fragment, (e) negatively charged G_4 dendrimer and (f) positively charged G_4 dendrimer.

experimentally at concentrations of 1 mg ml^{-1} [14]. The resulting amorphous cell containing both the positively and negatively charged dendrimers is shown in Figure 4.

(6) The energy of the resulting amorphous cell was minimised using the *smart minimiser*. This method combines the following steps:
  - ○ *Steepest Descent*, quickly reduces energy. This step is composed mainly of the so-called *line search*, which modifies the coordinates to generate a new, lower-energy structure. The line search direction is defined along the direction of the local downhill gradient. It will quickly reduce the energy of the structure during the first few iterations. However, convergence will slow down considerably as the gradient approaches zero. It is used when the gradients are very large and the configurations are far from the minimum; typically for poorly refined crystallographic data, or for graphically built molecules [40].
  - ○ *Conjugate Gradient*, compares energy with previous iteration. This improves the line search direction by storing information from the previous iteration. It is chosen because the system is too large for storing and manipulating a second-derivative matrix. The time per iteration is longer than for steepest descents, but this is more than compensated for by efficient convergence [41,42].
  - ○ *Newton–Rhaphson,* when the system is close to zero potential. It requires computation and storage of second derivatives and thus is expensive in terms of computer resources. For this reason it is only recommended for systems with a maximum of 200 atoms. However, it has a small convergence radius but it is very efficient near the energy minimum [43].

(7) Applying all previous three steps in a cascading manner, adding to that the equilibrium values of bond lengths and angles, plus the force constants, Van-der-Waals radii and associated constants required to calculate the nonbonded interactions.

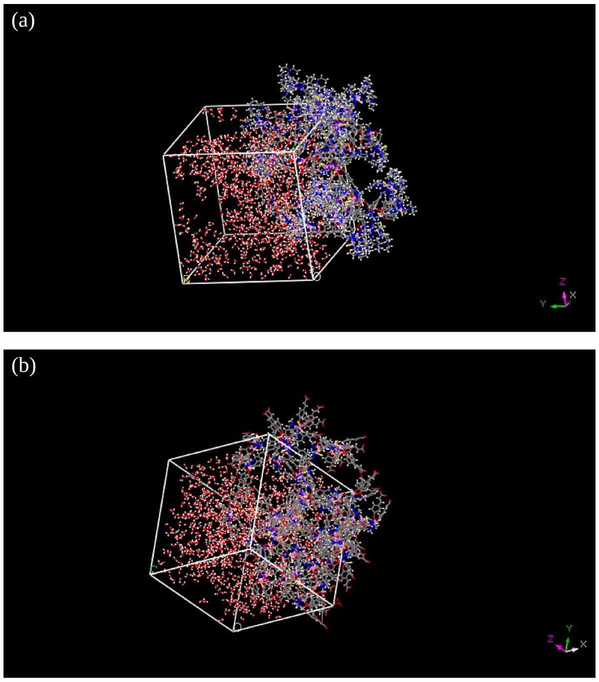

Figure 4. Amorphous cell of (a) G_4^+ and (b) G_4^- dendrimers in water.

3. Discussion

The combination of all previous parameters with the functional forms of the individual energy terms is known as a forcefield. Condensed-Phase Optimised Molecular Potentials for Atomistic Simulation Studies (COMPASS) is the forcefield used in the energy minimisation in the present report. It is an *ab initio* based forcefield that was parameterised using extensive data for molecules in the condensed phase. It is able to make accurate predictions of structural, conformational, and vibrational properties for a broad range of compounds, especially polymers, both in isolation and in condensed phases [33–36,38,39].

The coordinates of a structure combined with the COMPASS forcefield create an *energy expression*. This energy expression is the equation that describes the potential energy surface of a particular structure as a function of its atomic coordinates.

The potential energy in this case can be expressed as a sum of valence (or bond), cross term and non-bond interactions as represented in Equation (1):

$$E_{\text{total}} = E_{\text{valence}} + E_{\text{crossterm}} + E_{\text{non-bond}} \tag{1}$$

The energy of *valence* interactions is generally accounted for by bond stretching, valence angle bending, dihedral angle torsion and inversion, also called out-of-plane (oop) interactions terms, which are part of the forcefield for covalent systems and the Urey–Bradley (UB) term may be used to account for interactions between atom pairs involved in 1–3 configurations, i.e. atoms bound to a common atom. This is represented in Equation (2):

$$E_{\text{valence}} = E_{\text{bond}} + E_{\text{angle}} + E_{\text{torsion}} + E_{\text{oop}} + E_{\text{UB}} \tag{2}$$

Cross terms are used to account for factors as bond or angle distortions caused by nearby atoms. These terms are required to accurately reproduce experimental vibrational frequencies and, therefore, the dynamic properties of molecules. Cross terms can include stretch—stretch, stretch–bend–stretch, bend–bend, torsion–stretch, torsion–bend–bend, bend–torsion–bend, and stretch–torsion–stretch. *Non-bond* interactions are accounted for by Van der Waals, electrostatic (Coulomb) and hydrogen bond terms, represented in Equation (3):

$$E_{\text{non-bond}} = E_{\text{vdW}} + E_{\text{Coulomb}} + E_{\text{hbond}} \tag{3}$$

As an example for the complete energy expression, for water molecules we consider the following Equation (4), which might be used to describe the potential energy surface of a water structure:

$$\begin{aligned} V(R) = {} & K_{\text{oh}}(b - b^0_{\text{oh}})^2 + K_{\text{oh}}\left(b' - b^0_{\text{oh}}\right)^2 \\ & + K_{\text{hoh}}\left(\theta - \theta^0_{\text{hoh}}\right) \end{aligned} \tag{4}$$

The forcefield defines the bond lengths (b) and angles (θ), the functional form (a simple quadratic in both types of coordinates, the force constants (K), the reference O—H bond length (b^0) and H—O—H angle (θ^0) are the values for an ideal O—H bond and H—O—H angle at zero energy, which is not necessarily the same as their equilibrium values in a real water molecule.

The expression corresponding to the general, summed forcefield function can be written as follows:

$$\begin{aligned} V(R) = {} & \sum_b D_b[1 - \exp(-a(b - b_0))]^2 + \sum_\theta H_\theta(\theta - \theta_0)^2 \\ & + \sum_\phi H_\phi[1 + s\cos(n\phi)] + \sum_\chi H_\chi \chi^2 \\ & + \sum_b \sum_{b'} Fbb'(b - b_0)(b' - b'_0) \\ & + \sum_\theta \sum_{\theta'} F\theta\theta'(\theta - \theta_0)(\theta' - \theta'_0) \\ & + \sum_b \sum_\theta F_{b\theta}(b - b_0)(\theta - \theta_0) \\ & + \sum_\theta \sum_{\theta'} F_{\theta\theta'\phi}(\theta - \theta_0)(\theta' - \theta'_0)\cos\phi \\ & + \sum_\chi \sum_{\chi'} F_{\chi\chi'}\chi\chi' + \sum_i \sum_{j>i} \left[\frac{A_{ij}}{r_{ij}^{12}} - \frac{B_{ij}}{r_{ij}^6} + \frac{q_i q_j}{r_{ij}}\right] \end{aligned} \tag{5}$$

The first four terms in Equation (5) are sums that reflect the energy needed to stretch bonds (b), bend angles (θ) away from their reference values, rotate torsion angles (ϕ) by twisting atoms about the bond axis that determines the torsion angle and distort planar atoms out of the plane formed by the atoms they are bonded to (χ).

The next five terms in Equation (5) are cross terms that account for interactions between the four types of internal coordinates.

The final term in Equation (5) represents the non-bond interactions as a sum of repulsive and attractive Lennard-Jones terms as well as Coulombic terms, all of which are a function of the distance (r_{ij}) between atom pairs.

All these terms are included in the COMPASS forcefield were validated in earlier studies [44–47] and used in the accelrys software. More mathematical details are not shown here for simplicity but can be referred to on the Accelrys website (www.accelrys.com) and in the help menu of Materials Studio and other related software e.g. Cerius^2. They are also dealt with in more detail during the validation studies of the forcefield [44–47].

Values of bond lengths, bond angles, dihedral angles as well as exact co-ordinates of each atom are always saved in a special file during the energy minimisation process. Initial values are consistent with those reported in the literature [48–51]. The resulting structure after energy minimisation procedure explained above for the positively and negatively charged dendrimers is shown in Figures 5 and 6. Five thousand iterations were applied to minimise the energy. Only the scale of 200 iterations is shown in the graphs (Figure 5(a) and Figure 6(a)) for clarity and simplicity purposes. This shows how the *steepest descent* method and the *conjugate gradient* method were used efficiently to reduce the potential energy of the amorphous cell to approach zero. The *Newton–Ralphson* method was used afterwards to refine the structure.

4. Conclusion

Materials Studio was used efficiently to build a dendrimer/water amorphous cell. It allowed us to minimise the energy of the resulting structure and study the actual behaviour in water. This system is of extreme importance for bio-sensing and will be explored further in order to examine the behaviour of the system in the presence of counter ions. The model obtained so far shows that these dendrimers under investigation are not completely spherical as they were first regarded. Also the long branches tend to bend giving the dendrimer a diameter of *ca* ~1–3 nm, depending on the degree of collapse of the chains, which is in good agreement with Surface Plasmon Resonance and Quartz Crystal Microbalance with Dissipation experimental studies performed in our group [13,14,52]. We are in the process of not only

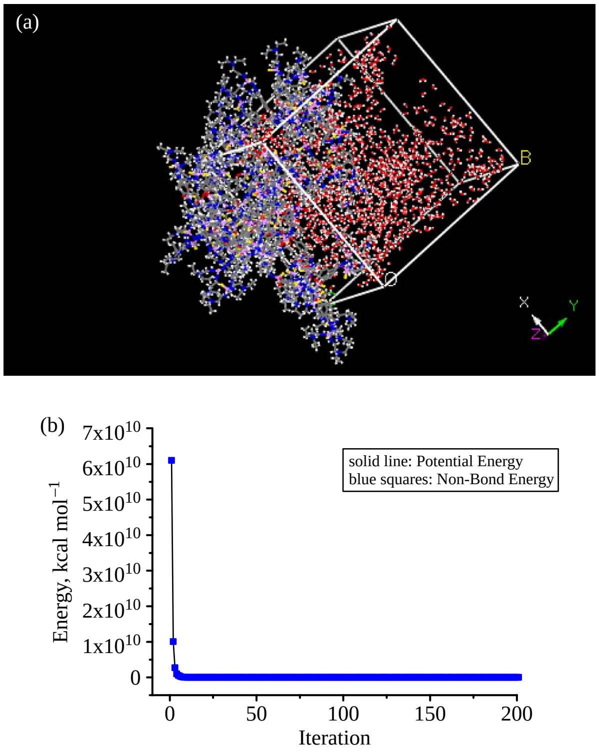

Figure 5. (a) Structure of G_4^+ after energy minimisation and (b) energy vs. number of iterations diagram showing the energy difference between the start and end structures.

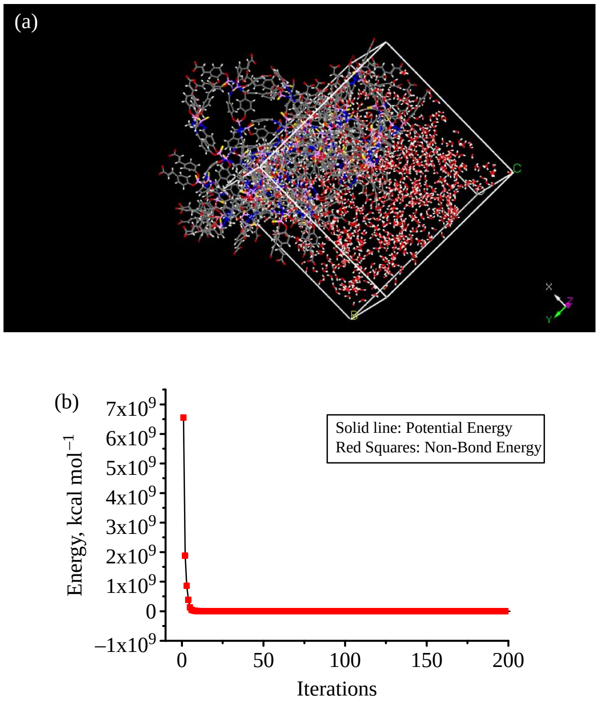

Figure 6. (a) Structure of G_4^- after energy minimisation and (b) energy vs. number of iterations diagram showing the energy difference between the start and end structures.

validating experimental data using Materials Studio but of predicting the structures and their behaviour to suit our experimental needs.

Acknowledgements

A.I. Abou-Kandil would like to thank Drs Alexandra Simperler and Carsten Menke from Accelrys for their initial help with Materials Studio setup. Funding from the IDB during the period from January 2007 until December 2007 is greatly appreciated.

References

[1] N. Launay, A.-M. Caminade, R. Lahana, and J.-P. Majoral, *Ein allgemeiner Zugang zu neutralen, phosphorhaltigen Dendrimeren*, Angew. Chem. 106(15/16) (1994), p. 1682.

[2] M. Wesolek, D. Meyer, J.A. Osborn, A. De Cian, J. Fischer, A. Derory, P. Legoll, and M. Drillon, *Ferromagneto-structural correlations in $[Mn(OC,X,H,),(bipy)]$ compounds, $X = C1$, Br*, Angew. Chem. Int. Ed. Eng. 33(15/16) (1994), p. 1529.

[3] J.-P. Majoral and A.-M. Caminade, *Dendrimers containing heteroatoms (Si, P, B, Ge, or Bi)*, Chem. Rev. 99 (1999), p. 845.

[4] M.-L. Lartigue, M. Slany, A.-M. Caminade, and J.-P. Majoral, *Phosphorus-containing dendrimers: Synthesis of macromolecules with multiple tri- and tetrafunctionalization*, Chem. Eur. J. 2(11) (1996), p. 1417.

[5] N. Launay, M. Slany, A.-M. Caminade, and J.-P. Majoral, *Phosphorus-containing dendrimers: Easy access to new multi-difunctionalized macromolecules*, J. Org. Chem. 61 (1996), p. 3799.

[6] L. Routaboul, S. Vincendeau, C.-O. Turrin, A.-M. Caminade, J.-P. Majoral, J.-C. Daran, and E. Manoury, *New phosphorus dendrimers with chiral ferrocenyl phosphine-thioether ligands on the periphery for asymmetric catalysis*, J. Organo'met. Chem. 692 (2007), p. 1064.

[7] P. Servin, C. Rebout, R. Laurent, M. Peruzzini, A.-M. Caminadea, and J.-P. Majoral, *Reduced number of steps for the synthesis of dense and highly functionalized dendrimers*, Tetrahed. Lett. 48 (2007), p. 579.

[8] L. Brauge, G. Veriot, G. Franc, R. Deloncle, A.-M. Caminadea, and J.-P. Majoral, *Synthesis of phosphorus dendrimers bearing chromophoric end groups: Toward organic blue light-emitting diodes*, Tetrahed. 62 (2006), p. 11891.

[9] A.-M. Caminade and J.-P. Majoral, *Nanomaterials based on phosphorus dendrimers*, Acc. Chem. Res. 37(6) (2004), p. 341.

[10] D.H. Kim, J.L. Mernandez-Lopez, J. Liu, G. Mihov, L. Zhi, R.E. Bauer, D. Grebel-Kohler, M. Klaffer, T. Weil, K. Mullem, et al., *Multilayer films fabricated from oppositely charged polyphenylene dendrimers by electrostatic Layer-by-Layer Assembly*, Macromol. Chem. Phys. 206 (2005), p. 52.

[11] B-S. Kim, O.V. Lebedeva, D.H. Kim, A.-M. Caminade, J.-P. Majoral, W. Knoll, and O.I. Vinogradova, *Assembly and mechanical properties of phosphorus dendrimer/polyelectrolyte multilayer microcapsules*, Langmuir 21(16) (2005), p. 7200.

[12] Z. Liang, A.S. Susha, A. Yu, and F. Caruso, *Nanotubes prepared by layer-by-layer coating of porous membrane templates*, Adv. Mater. 15(21) (2003), p. 1849.

[13] D.H. Kim, P. Karan, P. Gçring, J. Leclaire, A.-M. Caminade, J.-P. Majoral, U. Gçsele, M. Steinhart, and W. Knoll, *Formation of dendrimer nanotubes by Layer-by-Layer deposition*, Small 1(1) (2005), p. 99.

[14] C.-L. Feng, X. Zhong, M. Steinhart, A.-M. Caminade, J.-P. Majoral, and W. Knoll, *Graded-bandgap quantum-dot-modified nanotubes: A sensitive biosensor for enhanced detection of DNA hybridization*, Adv. Mater. 19 (2007), p. 1933.

[15] S. Merino, L. Brauge, A.M. Caminade, J.P. Majoral, D. Taton, and Y. Gnanou, *Synthesis and characterization of linear, hyperbranched, and dendrimer-like polymers constituted of the same repeating unit*, Chem. Eur. J. 7 (2001), p. 3095.

[16] A. Mecke, I. Lee, J.R. Baker Jr., M.M. Banaszak Holl, and B.G. Orr, *Deformability of poly(amidoamine) dendrimers*, Eur. Phys. J.E. 14 (2004), p. 7.

[17] Z. Balogh and I. Palinko, *Building dendrimer-like structures from a-phenyl pyrimidylcinnamic acid—a molecular modeling approach*, J. Mol. Struct. (Theochem) 623 (2003), p. 11.

[18] K.T. Welch, S. Arevalo, J.F.C. Turner, and R. Gomez, *An NMR and molecular modeling study of carbosilane-based dendrimers functionalized with phenolic groups or titanium complexes at the periphery*, Chem. Eur. J. 11 (2005), p. 1217.

[19] S. Rosenfeldt, E. Karpuk, M. Lehmann, H. Meier, P. Lindner, L. Harnau, and M. Ballauff, *The solution structure of stilbenoid dendrimers: A small-angle scattering study*, Chem. Phys. Chem. 7 (2006), p. 2097.

[20] S. Shinoda, M. Ohashi, and H. Tsukube, *Pocket Dendrimers" as nanoscale receptors for bimolecular guest accommodation*, Chem. Eur. J. 13 (2007), p. 81.

[21] J. J. Khandare, S. Jayant, A. Singh, P. Chandna, Y. Wang, N. Vorsa, and T. Minko, *Dendrimer versus linear conjugate: Influence of polymeric architecture on the delivery and anticancer effect of paclitaxel*, Bioconjugate Chem. 17 (2006), p. 1464.

[22] D.B. Amabilino, P.R. Ashton, V. Balzani, C.L. Brown, A. Cred, J.M.J. Frechet, J.W. Leon, F.M. Rayno, N. Spencer, J.F. Stoddart, et al., *Self-assembly of [n]rotaxanes bearing dendritic stoppers*, J. Am. Chem. Soc. 118 (1996), p. 12012.

[23] D.J. Diaz, G.D. Storrier, S. Bernhard, K. Takada, and H.D. Abruna, *Ordered arrays generated via metal-initiated self-assembly of terpyridine containing dendrimers and bridging ligands*, Langmuir 15 (1999), p. 7351.

[24] D.J. Diaz, S. Bernhard, G.D. Storrier, and H.D. Abruna, *Redox active ordered arrays via metal initiated self-assembly of terpyridine based ligands*, J. Phys. Chem. B 105 (2001), p. 8746.

[25] S. Granick, S.K. Kumar, E.J. Amis, M. Antonietti, A.C. Balazs, A.K. Chakraborty, G.S. Gress, C. Hawker, P. Janmey, et al., *Macromolecules at surfaces: Research challenges and opportunities from tribology to biology*, J. Polym. Sci. Part B: Polym. Phys. 41 (2003), p. 2755.

[26] Y. Choi, A. Mecke, B.G. Orr, M.M. Banaszak Holl, and J.R. Baker, Jr., *DNA-directed synthesis of generation 7 and 5 PAMAM dendrimer nanoclusters*, Nano Lett. 4(3) (2004), p. 391.

[27] I. Bury, B. Heinrich, C. Bourgogne, D. Guillon, and B. Donnio, *Supramolecular self-organization of "Janus-like" diblock codendrimers: Synthesis, thermal behaviour, and phase structure modeling*, Chem. Eur. J. 12 (2006), p. 8396.

[28] S. Fomine, L. Fomina, and P. Guadarrama, *Synthesis, properties and molecular modeling of functional hyperbranched polymers and dendrimers, Macromol.* Symp. 192 (2003), p. 43.

[29] I. Tsogas, D. Tsiourvas, G. Nounesis, and C.M. Paleos, *Modeling cell membrane transport: Interaction of guanidinylated poly (propyleneimine) dendrimers with a liposomal membrane consisting of phosphate-based lipids*, Langmuir 22 (2006), p. 11322.

[30] T.J. Prosa, B.J. Bauer, E.J. Amis, D.A. Tomalia, and R. Scherrenber, *A SAXS study of the internal structure of dendritic polymer systems*, J. Polym. Sci. Part B: Polym. Phys. 35 (1997), p. 2913.

[31] F.M. Menger, A.V. Peresypkin, and S. Wu, *Do dendritic amphiphiles self-assemble in water? A Fourier transform pulse-gradient spin-echo NMR study*, J. Phys. Org. Chem. 14 (2001), p. 392.

[32] T. Cagin, G. Wang, R. Martin, G. Zamanakos, N. Vaidehi, D.T. Mainz, and W.A. Goddard III, *Multiscale modeling and simulation methods with applications to dendritic polymers*, Comp. Theor. Polym. Sci. 11 (2001), p. 345.

[33] A.I. Abou-Kandil, G. Goldbeck-Wood, and A.H. Windle, *Molecular modeling of the intermediate smectic mesophase in polyethylene terephthalate*, Macromolecules 40(18) (2007), p. 6448.

[34] S. Pricl and M. Fermeglia, *Molecular simulation of host ± guest inclusion compounds: An approach to the lactodendrimers case*, Carbohyd. Polym. 45 (2001), p. 23.

[35] L. Metullio, M. Ferrone, A. Coslanich, S. Fuchs, M. Fermeglia, M.S. Paneni, and S. Pricl, *Polyamidoamine (yet not PAMAM) dendrimers as bioinspired materials for drug delivery: Structure-activity relationships by molecular simulations*, Biomacromolecules 5 (2004), p. 1371.

[36] W. Ortiz, A.E. Roitberg, and J.L. Krause, *Molecular dynamics of poly(benzylphenyl ether) dendrimers: Effects of backfolding on forster energy-transfer rates*, J. Phys. Chem. B 108 (2004), p. 8218.

[37] S. Zhang, Y. Rio, F. Cardinali, C. Bourgogne, J.-L. Gallani, and J.-F. Nierengarten, *Amphiphilic diblock dendrimers with a fullerene cor*, J. Org. Chem. 68 (2003), p. 9787.

[38] K. Yin, D. Zou, J. Zhong, D. Xu, *A new method for calculation of elastic properties of anisotropic material by constant pressure molecular dynamics*, Comput. Mater. Sci. 38 (2007), p. 538.

[39] M. Grujicic, Y.-P. Sun, and K.L. Koudela, *The effect of covalent functionalization of carbon nanotube reinforcements on the atomic-level mechanical properties of poly-vinyl-ester-epoxy*, Appl. Surf. Sci. 253 (2007), p. 3009.

[40] M. Levitt and S. Lifson, *Refinement of protein conformations using a macromolecular energy minimization procedure*, J. Mol. Biol. 46 (1969), p. 269.

[41] R. Fletcher and C.M. Reeves, *Function minimization by conjugate gradients*, Comput. J. 7(2) (1964), p. 149.

[42] W.H. Press, B.P. Flannery, S.A. Teukolsky, and W.T. Vetterling, *Numerical Recipes, The Art of Scientific Computing*, Cambridge University Press, Cambridge, 1986.

[43] O. Ermer, *Calculation of molecular properties using force fields. Applications in organic chemistry*, Struct. Bond. 27 (1976), p. 161.

[44] H. Sun, *COMPASS: An ab initio force-field optimized for condensed-phase applications-overview with details on alkane and benzene compounds*, J. Phys. Chem. B. 102 (1998), p. 7338.

[45] H. Sun and D. Rigby, *Polysiloxanes: Ab initio force field and structural, conformational and thermophysical properties*, Spectrochimica Acta A 53 (1997), p. 1301.

[46] D. Rigby and H. Sun, and B.E. Eichinger, *Computer simulations of poly(ethylene oxide): Force field, pvt diagram and cyclization behaviour*, Polymer International 44 (1997), p. 311.

[47] T. Spyriouni and C. Vergelati, *A molecular modeling study of binary blend compatibility of polyamide 6 and poly(vinyl acetate) with different degrees of hydrolysis: an atomistic and mesoscopic approach*, Macromolecules 34 (2001), p. 5306.

[48] M.-L. Lartigue, B. Donnadieu, C. Galliot, A.-M. Caminade, J.-P. Majoral, and J.-P. Fayet, *Large dipole moments of phosphorus-containing dendrimers*, Macromolecules 30 (1997), p. 7335.

[49] C. Larre, B. Donnadieu, A.-M. Caminade, and J.-P. Majoral, *Phosphorus-containing dendrimers: Chemoselective functionalization of internal layers*, J. Am. Chem. Soc. 120 (1998), p. 4029.

[50] C. Larre, D. Bressolles, C. Turrin, B. Dommadieu, A.-M. Caminade, and J.-P. Majoral, *Chemistry within megamolecules: Regiospecific functionalization after construction of phosphorus dendrimers*, J. Am. Chem. Soc. 120 (1998), p. 13070.

[51] V. Maraval, R. Laurent, B. Donnadieu, M. Mauzac, A.-M. Caminade, and J.-P. Majoral, *Rapid synthesis of phosphorus-containing dendrimers with controlled molecular architectures: First example of surface-block, layer-block, and segment-block dendrimers issued from the same dendron*, J. Am. Chem. Soc. 122 (2000), p. 2499.

[52] A.I. Abou-Kandil and W. Knoll, in preparation